Utilization of Citric Acid to Improve the Depressive Efficiency of Sodium Silicate on the Flotation of Calcite and Fluorite

Yu Wang[1] · Xi Zhang[1] · Jie Zhang[1] · Wei Zhao[1]

Abstract

As a common depressant of calcite and fluorite, sodium silicate presents the disadvantages of large dosage and incomplete depression effect. Improving the depression effect of sodium silicate on calcite and fluorite, reducing the amount of sodium silicate in mineral processing is of great industrial and economic importance. In this manuscript, a novel reagent scheme is proposed that adding a small amount of citric acid (CA) can greatly improve the depression effect of sodium silicate on calcite and fluorite. The flotation results suggest that the CA concentration to be added is 4×10^{-4} mol/L and the sodium silicate concentration is 5×10^{-3} mol/L; the recoveries of calcite and fluorite reach 0.9% and 1.1%, suggesting the two minerals have been depressed, completely. Theoretical analysis results indicate that the addition of CA dissolves calcium ions of the calcite and fluorite surface and decreases the calcium activation sites on the mineral surface. Then, the addition of sodium silicate adsorbs on the remaining calcium sites on the calcite and fluorite surfaces, further preventing the collector adsorbed on the mineral surfaces. DFT calculation further proves the depression mechanism of mixed depressant that sodium silicate is easy to adsorb on the surface of calcite and fluorite surfaces, while citric acid is difficult to adsorb on the surface of calcite and fluorite surfaces.

Keywords Calcite · Fluorite · Mixed depressant · Flotation · Sodium silicate · Citric acid

1 Introduction

Fluorite and calcite, as the most common calcium minerals, usually coexisted with other minerals such as scheelite, lead–zinc sulfide, and rare earth [1, 2]. High-purity fluorite and calcite have a wide range of industrial demands [3, 4]. However, low-grade fluorite and calcite seriously affected the concentrate grade in the flotation process [5–7]. As such, removing low-grade fluorite and calcite from target minerals in mineral processing was of great industrial and economic importance [8, 9].

Flotation was an effective approach for the separation of impurity minerals from valuable minerals [10, 11]. In general, the surface properties of minerals such as hydrophilicity changed observably by adding the depressants into the pulp to achieve the efficient depression effect [12, 13]. Hydroxypropyl starch, tartaric acid, carboxymethyl cellulose, and sodium silicate were the most common depressants of calcite and fluorite [13, 14]. In contrast, sodium silicate was one of the most popular depressants [15]. As a result of the depressant sodium silicate, hydrophilic precipitates of calcium silicate were formed on the surface of fluorite and calcite that hydrosoluble sodium silicate components reacted with calcium ions to extrude the collector on the surface [16]. Meanwhile, the depression effect of sodium silicate on the fluorite was better under alkaline conditions [17, 18].

In reality, single calcium mineral depressants often exhibit some disadvantages, such as weak depressive power and high consumption of reagents because of similar surface properties of calcium minerals and high reactivity with their conventional reagents [7, 19]. Developing and utilizing efficient depressants, such as the combination of depressants and modified depressants, were the key to alleviating such problems [20]. Using a mixture of sodium silicate and Pb^{2+} as depressants, Feng et al. [21] successfully separated scheelite from calcite by flotation. Pb^{2+} reacted with sodium silicate, which was more likely to adsorb on the surfaces of

✉ Xi Zhang
zhangxi0196@163.com

1   School of Chemical and Environmental Engineering, China University of Mining & Technology (Beijing), Yifu 214, D11, Xueyuan Road, Haidian District, Beijing 100083, China

calcite and scheelite. The pre-adsorption of sodium silicate interfered with the adsorption of benzohydroxamic acid on the calcite surface and depressed the flotation. The combination of Pb^{2+} and sodium silicate resulted in a significant reduction of the sodium silicate amount and an increase in the depression effect. Phosphates are widely used as a depressant for calcium minerals. This depressant is effective in increasing flotation selectivity, but the depressant usually causes serious issues, such as polluting the ecosystem and reducing the filtration speed of the tailings [22]. In addition, citric acid (CA) as a common anionic organic acid is widely used in various industries [23, 24], and the CA as one of the environmentally friendly agents had been studied as a depressant in mineral flotation [25]. For example, the mixture of CA and Fe^{3+} could be used as an effective depressant for calcite using sodium oleate (NaOL) as collectors [26]. Experiments indicate that the Fe^{3+} species in the slurry reacted with citric acid first and then co-adsorbed on the calcium atomic sites on the calcite surface. On the other hand, the Fe^{3+} species was first adsorbed on the oxygen atom sites on the surface of the calcite, and then the Fe^{3+} species provided the adsorption sites for further adsorption of citric acid. As a result, the dosage of CA decreased, significantly. In summary, it could be found that combined depressants could greatly improve the depression effect of depressants and effectively reduce the dosage of agents.

In this manuscript, the depressive performance of sodium silicate and CA on calcite and fluorite was investigated via flotation experiments. Based on this, the depression mechanism of the mixed depressant CA/sodium silicate was revealed via Zeta potential measurement, ICP experiments, DFT computation, and adsorption experiments. This work presented an efficient and economically feasible approach for removing calcite and fluorite from target minerals. In addition, the investigation effectively lessens the dosage of agents, reduces environmental pollution significantly, and improves the depression effect of sodium silicate on calcite and fluorite. This study provided an important theoretical basis for the development of new depressants.

2 Experimental

2.1 Minerals and Reagents

The high-grade fluorite and calcite samples used in this study were acquired from Yunnan, China. A series of processes, including manual selection, crushing, grinding, and sieving, were used to obtain the pure samples in the range of 74 to 38 μm. Analytical grade sodium oleate (NaOL), hydrochloric acid (HCl), sodium hydroxide (NaOH), sodium silicate, and CA purchased from Shanghai Macklin Biochemical Co., Ltd were used as the collector, pH regulators,

and depressants, respectively. In addition, terpineol was used as frother.

2.2 Flotation Experiments

The XFG laboratory flotation machine with a volume of 40 mL was carried out to float pure minerals and the impeller rotation speed was fixed at 1900 r/min. In the initial phase, 38 mL of deionized water and 2 g of fluorite or calcite samples were introduced to the flotation cell. Then, the pH of the mineral suspensions was adjusted by adding NaOH or HCl. Next, the collector and the depressant were subsequently added to the mineral suspensions and agitated for 2 min. Finally, terpineol oil was added as a frother. According to the weight distribution between the concentrates and tailings after artificial scraping, filtering, drying, and weighing, flotation recoveries for fluorite and calcite samples were calculated.

2.3 ICP-OES Experiments

The concentration of Ca^{2+} in the solution was investigated with an inductively coupled plasma emission spectrometer (ICP-OES). To begin, 2 g of the pure mineral was placed into a beaker containing 40 mL of deionized water and the mixture was stirred at 500 rpm with a magnetic stirrer. To achieve the ideal pH value, the pulp had to be adjusted during this process. Then, different agents were added to the beaker based on the dosing sequence of the flotation process, and they were stirred for a preset time. Finally, the concentration of calcium ions in the supernatant was measured to determine the dissolution of Ca ions on these surfaces.

2.4 Zeta potential measurements

Malvern Zetasizer Nano ZS90 was used to measure the zeta potential. Samples were freshly ground in an agate mortar to a size of − 2 um. For each experiment, 50 mg of the pure mineral was added to 40 mL of aqueous KCl solution to form a suspension. The concentration of KCl was fixed at 5×10^{-3} mol/L. Afterwards, reagents were added to the suspension, and it was stirred for several minutes. The suspension was then conditioned by magnetic stirring, during which reagents were added to the suspension and conditioned for a certain number of minutes. After standing for 10 min, the supernatant was removed and used for the zeta potential measurements. The final results were averaged over at least three repeated measurements.

2.5 Density Functional Theory (DFT) Calculations

The interaction models of depressants on mineral surfaces were performed using the CASTEP program [27, 28].

Generalized gradient approximation (GGA) using the Perdew–Wang generalized gradient approximation (PW91) functionals was adopted for the exchange–correlation functional, while ultra-soft pseudopotential was implemented to describe the electro-ion interactions [29, 30]. The valence electron configurations considered in the study were F $2s^2 2p^5$, Ca $3s^2 3p^6 4s^2$, and O $2s^2 2p^4$. Pre-tested plane-wave cutoff energy of 340 eV was used for all calculations, and *k*-space sampling was performed using the Monkhorst–Pack scheme. For self-consistent electronic minimization, the Pulay density mixing method was adopted with a convergence tolerance of 2.0×10^{-5} eV/atom. The convergence criteria for structure optimization and energy calculation were as follows: (a) energy tolerance of 2×10^{-5} eV/atom, (b) maximum force tolerance of 0.05 eV/Å, and (c) maximum stress of 0.1 GPa.

## 3 Results and Discussions

3.1 Flotation Experiments

The dosage of sodium silicate and pH value had to be determined before investigating the depression effect of sodium silicate and CA on calcite and fluorite. The effects of NaOL concentration and pH value on the floatability of fluorite and calcite are illustrated in Fig. 1a and Fig. 1b. From Fig. 1a, under natural pH, the NaOL displayed an excellent collecting ability for both fluorite and calcite, which is attributed to the chemisorption of NaOL on

fluorite and calcite [15, 16]. When the NaOL concentration reached 8×10^{-4} mol/L, the recoveries of fluorite and calcite reached 85.77% and 87.22%, respectively. With increasing concentrations of NaOL, the recoveries of fluorite and calcite remained almost constant. From Fig. 1b, the relatively low flotation recoveries of the two minerals at weakly acidic pH might be related to the Ca^{2+} produced by calcite and fluorite dissolution, causing the precipitation of NaOL and reducing the level of acid soap formation [31]. In addition, the flotation recoveries increased with the increase of pH, reaching the maximum at pH 9.5. The maximum recoveries of fluorite and calcite were 91.2% and 90.7%. As indicated, the optimal NaOL concentration and pH of fluorite and calcite flotation were fixed at 8×10^{-4} mol/L and 9.5, respectively.

Figure 1c and Fig. 1d displayed the effects of the single depressant (sodium silicate or CA) concentrations on the floatability of fluorite and calcite at the optimal condition. From Fig. 1c, the recoveries of fluorite and calcite decreased significantly when the sodium silicate concentration was increased from 5×10^{-4} to 5×10^{-3} mol/L. The recoveries of fluorite and calcite reached 24.3% and 14.3% when the sodium silicate concentration was 5×10^{-3} mol/L. With the increase of sodium silicate concentration, the recoveries of fluorite and calcite did not decrease significantly. From Fig. 1d, the recoveries of fluorite and calcite were influenced to a certain degree by a high CA concentration. The recoveries of fluorite and calcite decreased from 62.53% and 74.78% to 14.39% and 20.45% when the CA concentration increased from

Fig. 1 Effect of **a** NaOL concentration, **b** pH, **c** sodium silicate concentration, and **d** CA concentration on fluorite and calcite flotation
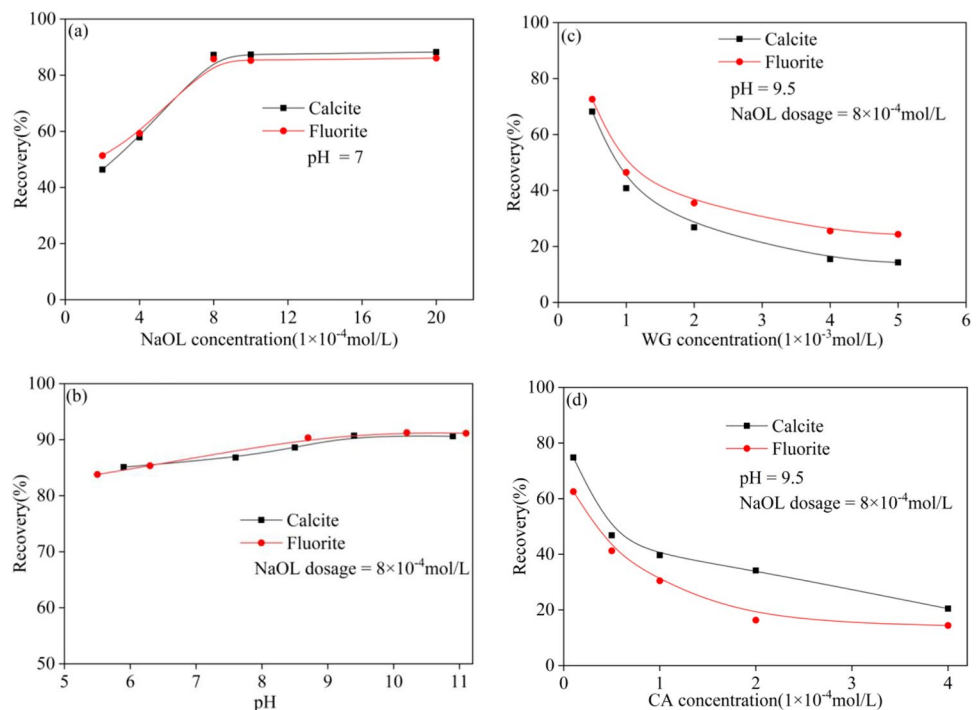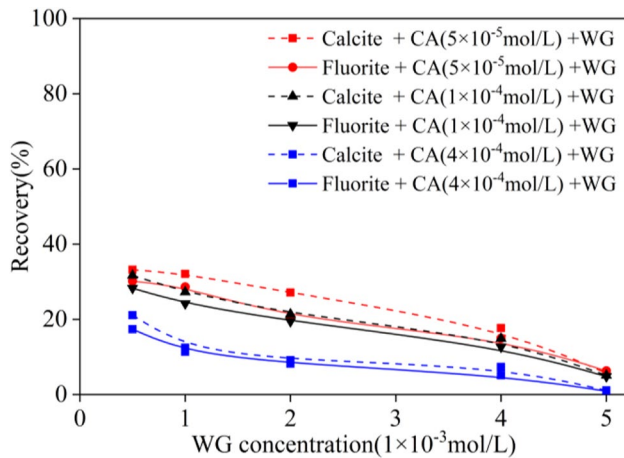
Fig. 2 Floatability of fluorite and calcite as a function of mixed depressant concentration

1×10^{-5} to 4×10^{-4} mol/L. Single depressant displayed a certain depressive effect on fluorite and calcite, while the dosage was large and the depressive effect was imperfect.

From Fig. 2, the recoveries of fluorite and calcite significantly decreased with the increase of mixed depressant (the mixture of CA and sodium silicate) dosage. When the concentration of CA was 5×10^{-5} mol/L, the recoveries of fluorite and calcite reached 30.1% and 33.1% at the sodium silicate concentration of 1×10^{-4} mol/L. However, at the sodium silicate concentration of 5×10^{-3} mol/L, the recoveries of fluorite and calcite were only 6.3% and 5.7%, respectively.

Furthermore, at a CA concentration of 4×10^{-4} mol/L, the recoveries of the two minerals further decreased with an increase in the sodium silicate concentration, and the recoveries of fluorite and calcite reached 0.9% and 1.1%, respectively, at the sodium silicate concentration of 5×10^{-3} mol/L. The results of flotation suggested that the depression effect of the mixed depressant CA/sodium silicate was more advantageous than that of the single depressant sodium silicate or CA.

3.2 Solution Chemical Calculation of CA Solution and Sodium Silicate Solution

The hydrosoluble component of the sodium silicate and CA solution affected the adsorption form of the flotation reagent on the mineral surface and further affected the floatability of fluorite and calcite. The equilibrium reaction formulas in sodium silicate and CA solutions are given in Table 1 [17, 26].

The formulas for calculating the distribution of sodium silicate and CA under different pH conditions were as follows:

Table 1 Reactions and corresponding reaction constants [17, 26]

Reactions	Reaction constants	
$SiO_{2(am)} + 2H_2O = H_4SiO_4$	$K_{sp} = 10^{-2.71}$	(1)
$H_2SiO_4^{2-} + H^+ = H_3SiO_4^-$	$K_1^H = 10^{12.56}$	(2)
$H_3SiO_4^- + H^+ = H_4SiO_4$	$K_2^H = 10^{9.43}$	(3)
$H^+ + CA^{3-} = CA^{2-}$	$K_{11}^H = 10^{6.396}$	(4)
$H^+ + CA^{2-} = CA^-$	$K_{12}^H = 10^{4.761}$	(5)
$H^+ + CA^- = CA$	$K_{13}^H = 10^{3.31}$	(6)

$$\alpha_{Si} = \alpha_{SiO_2(OH)_2^{2-}} + \alpha_{SiO(OH)_3^-} + \alpha_{Si(OH)_4} \tag{7}$$

$$\Phi_{SiO_2(OH)_2^{2-}} = 1/(1 + K_1^H[H^+] + K_1^H K_2^H[H^+]^2) \tag{8}$$

$$\Phi_{SiO(OH)_3^-} = K_1^H[H^+]\Phi_{SiO_2(OH)_2^{2-}} \tag{9}$$

$$\Phi_{Si(OH)_4} = K_2^H[H^+]^2\Phi_{SiO_2(OH)_2^{2-}} \tag{10}$$

$$\alpha_{CA^{3-}} = 1 + K_{11}^H[H^+] + K_{11}^H K_{12}^H[H^+]^2 + K_{11}^H K_{12}^H K_{13}^H[H^+]^3 \tag{11}$$

$$\Phi_{CA^{3-}} = 1/\alpha_{Cit^{3-}} = 1/(1 + K_{11}^H[H^+] + K_{11}^H K_{12}^H[H^+]^2 + K_{11}^H K_{12}^H K_{13}^H[H^+]^3) \tag{12}$$

$$\Phi_{CA^{2-}} = K_{11}^H[H^+]\Phi_{CA^{3-}} \tag{13}$$

$$\Phi_{CA^-} = K_{11}^H K_{12}^H[H^+]^2\Phi_{CA^{3-}} \tag{14}$$

$$\Phi_{CA} = K_{11}^H K_{12}^H K_{13}^H[H^+]^3\Phi_{CA^{3-}} \tag{15}$$

According to Formulas (1) to (15), the distribution coefficient of each component of sodium silicate solution and CA solution could be calculated, and the results are shown in Fig. 3.

As depicted in Fig. 3, the existing forms of sodium silicate in solution were mainly $Si(OH)_4$, $SiO(OH)_3^-$, and $SiO_2(OH)_2^{2-}$ components. When the pH gradually increased from 6 to 11, the component of $SiO(OH)_3^-$ in the solution gradually increased, and $Si(OH)_4$ gradually decreased. Furthermore, the hydrolysis and dissociation of CA in the solution produced CA, CA^-, CA^{2-}, and CA^{3-} substances. When the pH of the solution gradually increased from 4 to 10, the component of CA^{3-} in the solution gradually increased, and CA, CA^-, and CA^{2-} gradually decreased. Combined with the results of the flotation experiment, it could be found that sodium silicate mainly existed in the form of $SiO(OH)_3^-$ at pH 9.5, and CA mainly existed in the form of CA^{3-}.

**Fig. 3** Species distribution diagram of **a** sodium silicate and **b** CA in the solution as a function of pH
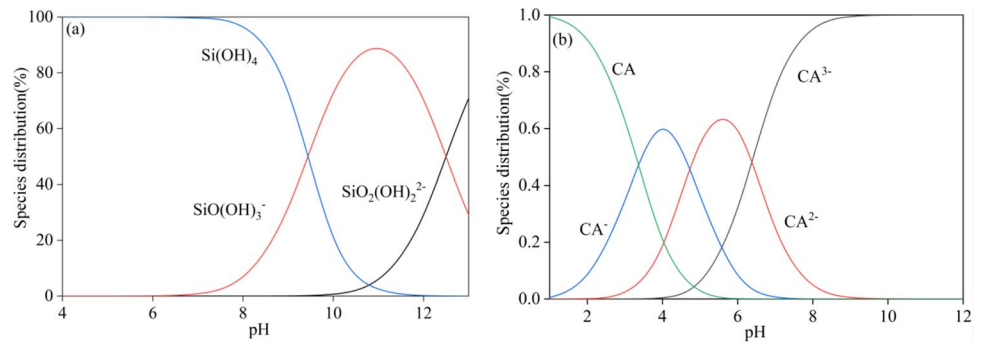
3.3 ICP Experiments

Flotation results indicate that calcite and fluorite were depressed strongly by the mixed depressant (CA/sodium silicate). To investigate the mechanism of sodium silicate and CA on the fluorite and calcite surfaces, the dissolution of Ca^{2+} on calcite and fluorite surfaces was analyzed, and the results are shown in Fig. 4. From Fig. 4a, the Ca^{2+} solubility of calcite and fluorite surfaces decreased gradually with the increase of sodium silicate concentration, due to the sodium silicate specific adsorption capacity on minerals and the reduced Ca^{2+} solubility [32]. From Fig. 4b, the Ca^{2+} solubility of calcite and fluorite surfaces increased gradually with the increase of CA concentration, suggesting that CA could reduce the Ca^{2+} on the calcite and fluorite surfaces. Combined with the results of flotation experiments and solution chemical calculations, it could be found that sodium silicate might adsorb on the surface of calcium-containing minerals.

3.4 Zeta Potential Experiments

Figure 5 gives the results of zeta potential measurements on fluorite and calcite with different reagent schemes. From Fig. 5, calcite and fluorite exhibited an isoelectric point at pH 8.8 and pH 8.2, respectively, which were in the range of previous reports [18]. As a result, sodium silicate displayed an obvious effect on calcite and fluorite surfaces. Sodium silicate significantly reduced the zeta potential for calcite and fluorite with an average decline of 40 mV and 30 mV in the pH range of 4–10, respectively, suggesting that sodium silicate adsorbed on the surfaces of calcite and fluorite. However, CA reduced the zeta potential for calcite and fluorite with an average decline of 4 mV and 2 mV in the pH range of 4–10, respectively, suggesting that that CA did not favorably adsorb on the surfaces of calcite and fluorite. Moreover, the results indicated that CA dissolved the calcium activation sites on the mineral's surface, resulting in a decrease in the amount of the collector on the calcite and fluorite surfaces, as well as sodium silicate adsorbed on the

Fig. 4 Dissolution of Ca^{2+} with different **a** sodium silicate and **b** CA concentrations
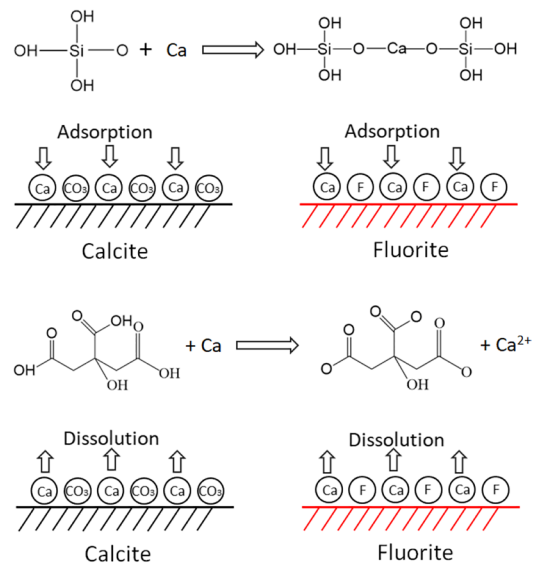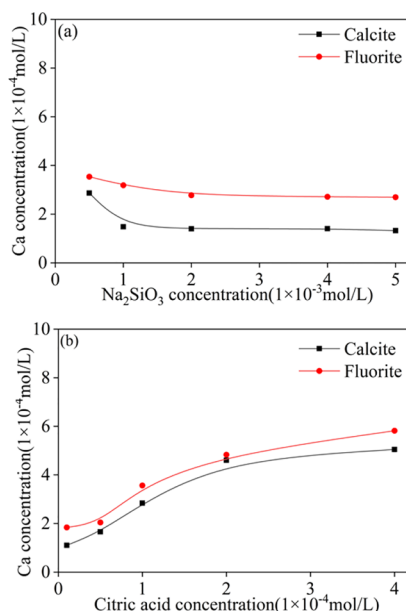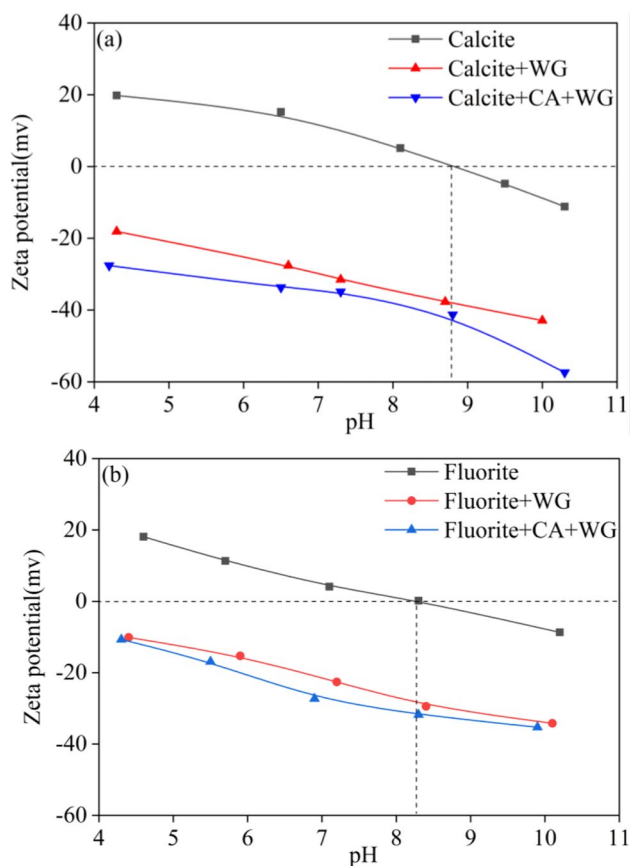
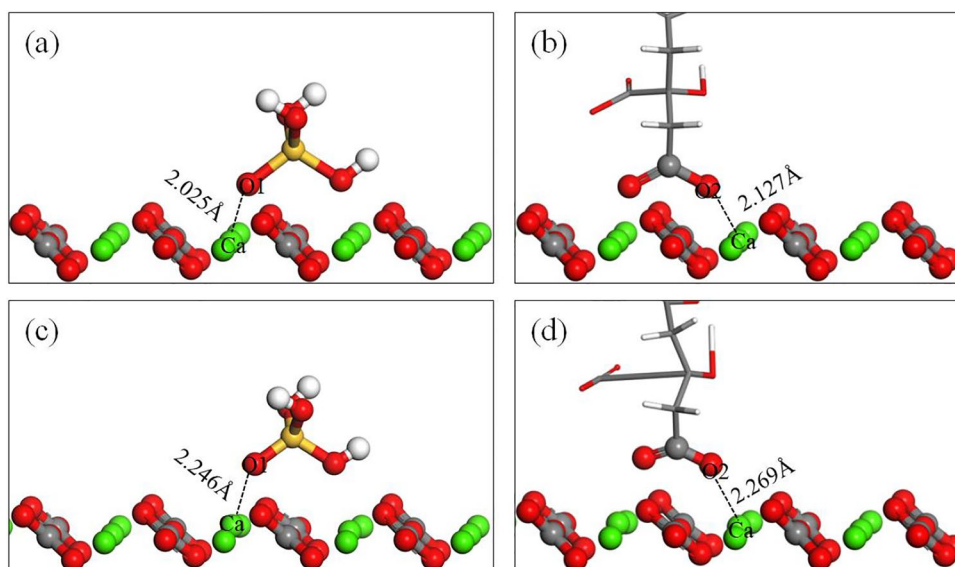Fig. 5 Zeta potentials of calcite and fluorite with different reagents

surface of calcium minerals, which impeded the adsorption of the collector.

3.5 DFT Calculation

Firstly, a $(3 \times 3 \times 1)$ super-cell of fluorite and calcite was constructed, and geometry optimization was performed. The cleavage planes of fluorite and calcite were the fluorite (111) surface and calcite (104) surface [33, 34]. Then, CA^{3-} and $SiO(OH)_3^-$ were situated on the mineral's surface, and the interaction was simulated. The interaction models are shown in Fig. 6 and Fig. 7.

Density functional theory (DFT) of quantum mechanics was used to simulate the adsorption of $SiO(OH)_3^-$ and CA^{3-} on the calcite (104) surface. Figure 6 presented the models of $SiO(OH)_3^-$ and CA^{3-} interaction with the calcite (104) surface. $SiO(OH)_3^-$ and CA^{3-} were perpendicularly placed on the calcite (104) surface. Initial distances of Ca-O1 and Ca-O2 bonds were 2.025 Å and 2.127 Å for Fig. 6a and Fig. 6b, respectively, which were less than the sum of the radii of the O atom and Ca atom. As shown in Fig. 6c and Fig. 6d, after CA^{3-} and $SiO(OH)_3^-$ interacted with the calcite (104) surface, the Ca-O1 bond length was 2.246 Å, which was smaller than the sum of the radii of Ca and O (2.63 Å). Similarly, in the case of CA^{3-} interacting with Ca atom on the calcite (104) surface, the Ca-O2 bond length was 2.496 Å, which was right in the bonding range. In addition, when $SiO(OH)_3^-$ and CA^{3-} were adsorbed on the calcite (104) surface, the adsorption energies were -17.33 eV and -0.54 eV respectively. The results suggested that the adsorption of $SiO(OH)_3^-$ on the calcite (104) surface was much stronger than the adsorption of CA on the calcite (104) surface. Figure 7 presents the models of $SiO(OH)_3^-$ and CA^{3-} interacted with the fluorite (111)

Fig. 6 The interaction models. **a** Before $SiO(OH)_3^-$ adsorption on the calcite (104) surface. **b** Before CA^{3-} adsorption on the calcite (104) surface. **c** After $SiO(OH)_3^-$ adsorption on the calcite (104). **d** After CA^{3-} adsorption on the calcite (104) surface

Fig. 7 The interaction models.
a Before $SiO(OH)_3^-$ adsorption on the fluorite (111) surface. **b** Before CA^{3-} adsorption on the fluorite (111) surface. **c** After $SiO(OH)_3^-$ adsorption on the fluorite (111) surface. **d** After CA^{3-} adsorption on the fluorite (111) surface
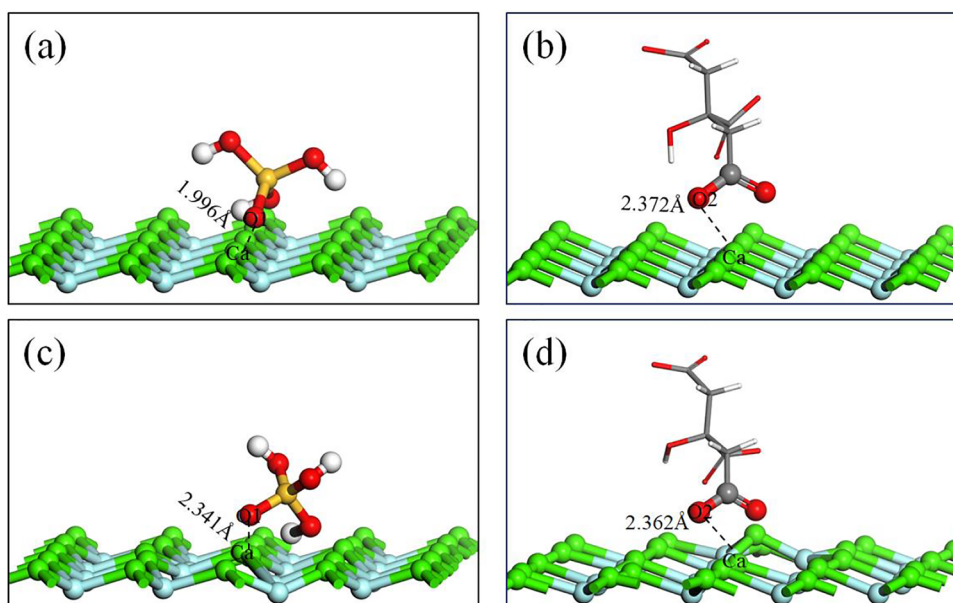
Table 2 Adsorption energy and bond length of sodium silicate and CA on mineral surfaces

Adsorption models	ΔE_{ads}, eV	Bonds	Distance before, Å	Distance after, Å
Calcite + sodium silicate	− 17.33	Ca-O1	2.025	2.246
Calcite + CA	− 0.54	Ca-O2	2.127	2.269
Fluorite + sodium silicate	− 10.19	Ca-O1	1.996	2.341
Fluorite + CA	− 6.06	Ca-O2	2.372	2.362

surface. $SiO(OH)_3^-$ and CA^{3-} were perpendicularly placed on the fluorite (111) surface. Initial distances of Ca-O1 and Ca-O2 bonds were 1.996 Å and 2.372 Å for Fig. 7a and Fig. 7b, respectively, which was less than the sum of the radii of the O atom and Ca atom. Similarly, in the case of CA^{3-} interacting with the Ca atom on the fluorite (111) surface, the Ca-O2 bond length was 2.362 Å, which was right in the bonding range. In addition, when $SiO(OH)_3^-$ and CA^{3-} are adsorbed on the fluorite (111) surface, the adsorption energies were − 10.19 eV and − 6.06 eV, respectively. The results suggested that the adsorption of $SiO(OH)_3^-$ on the calcite (104) surface was much stronger than the adsorption of CA on the fluorite (111) surface (Table 2).

4 Conclusions

Single mineral flotation results indicated that sodium silicate and CA presented a certain depressive effect on calcite and fluorite, and the depression effect of mixed depressants on calcite and fluorite was obviously better than that of a single depressant. When the concentration of CA was 4×10^{-4} mol/L and the sodium silicate concentration was 5×10^{-3} mol/L, the recoveries of calcite and fluorite reached 0.9% and 1.1%. The theoretical analysis results illustrated that the addition of CA dissolved calcium ions from the calcite and fluorite surface and decreased the calcium sites on the mineral surface. Next, the addition of sodium silicate adsorbed on the remaining calcium sites on the calcite and fluorite surfaces prevented the NaOL adsorbed on the mineral surfaces. The synergistic interaction of both CA and sodium silicate depicted a strong depression effect on calcite and fluorite. DFT calculation further illustrated that sodium silicate was easy to adsorb on the surface of calcite and fluorite surfaces, while citric acid was difficult to adsorb on the surface of calcite and fluorite surfaces.

Declarations

References

1. Chen J, Yang RD, Du LJ, Gao JB, Zheng LL, Huang ZL (2020) Multistage fluid sources and evolution of Qinglong Sb-(Au) deposit in northern margin of Youjiang basin, SW China: REE geochemistry and Sr-H-O isotopes of ore-related jasperoid, quartz and fluorite. Ore Geol Rev 127:103851. https://doi.org/10.1016/j.oregeorev.2020.103851

2. Mohamed MAM (2013) Evolution of mineralizing fluids of cassiterite-wolframite and fluorite deposits from Mueilha tin mine area, Eastern Desert of Egypt, evidence from fluid inclusion. Arab J Geosci 6:775–782. https://doi.org/10.1007/s12517-011-0402-8

3. Ishikawa K, Koga N, Tsuru K, Takahashi I (2016) Fabrication of interconnected porous calcite by bridging calcite granules with dicalcium phosphate dihydrate and their histological evaluation. J Biomed Mater Res - Part A 104:652–658. https://doi.org/10.1002/jbm.a.35604

4. Cao YY, Zhang Y (2019) Adsorption of H4SiO4 as a hydrolysate of sodium silicate on surfaces of fluorite (111), calcite (104), and scheelite (112): a density functional theory approach. Int J Electrochem Sci. 14:10807–10818. https://doi.org/10.20964/2019.12.78.

5. Wang J, Bai J, Yin W, Liang X (2018) Flotation separation of scheelite from calcite using carboxyl methyl cellulose as depressant. Miner Eng 127:329–333. https://doi.org/10.1016/j.mineng.2018.03.047

6. Zhou W, Moreno J, Torres R, Valle H, Song S (2013) Flotation of fluorite from ores by using acidized water glass as depressant. Miner Eng 45:142–145. https://doi.org/10.1016/j.mineng.2013.02.017

7. Deng R, Yang X, Hu Y, Ku J, Zuo W, Ma Y (2018) Effect of Fe(II) as assistant depressant on flotation separation of scheelite from calcite. Miner Eng 118:133–140. https://doi.org/10.1016/j.mineng.2017.12.017

8. Lai H, Deng J, Liu Q, Wen S, Song Q (2021) Surface chemistry investigation of froth flotation products of lead-zinc sulfide ore using ToF-SIMS and multivariate analysis. Sep Purif Technol 254:117655. https://doi.org/10.1016/j.seppur.2020.117655

9. Gao J, Hu Y, Sun W, Liu R, Gao Z, Han H, Lyu F, Jiang W (2019) Enhanced separation of fluorite from calcite in acidic condition. Miner Eng 133:103–105. https://doi.org/10.1016/j.mineng.2019.01.013

10. Chen Y, Tang X (2020) Selective flotation separation of smithsonite from calcite by application of amino trimethylene phosphonic acid as depressant. Appl Surf Sci 512:145663. https://doi.org/10.1016/j.apsusc.2020.145663

11 Gao ZY, Sun W, Hu YH, Liu XW (2012) Anisotropic surface broken bond properties and wettability of calcite and fluorite crystals. Trans Nonferrous Met Soc China (English Ed). 22:1203–1208. https://doi.org/10.1016/S1003-6326(11)61306-X

12. Chen S, Wen X, Huang S, Huang F, Cheng YB, Green M, Ho-Baillie A (2017) Light illumination induced photoluminescence enhancement and quenching in lead halide perovskite. Sol RRL 1:1–8. https://doi.org/10.1002/solr.201600001

13. Shi Q, Feng Q, Zhang G, Deng H (2014) A novel method to improve depressants actions on calcite flotation. Miner Eng 55:186–189. https://doi.org/10.1016/j.mineng.2013.10.010

14. Zhu H, Qin W, Chen C, Chai L, Jiao F, Jia W (2018) Flotation separation of fluorite from calcite using polyaspartate as depressant. Miner Eng 120:80–86. https://doi.org/10.1016/j.mineng.2018.02.016

15. Tang Y, Yin W, Kelebek S (2020) Selective flotation of magnesite from calcite using potassium cetyl phosphate as a collector in the presence of sodium silicate. Miner Eng 146:106154. https://doi.org/10.1016/j.mineng.2019.106154

16. Gao Z, Wang C, Sun W, Gao Y, Kowalczuk PB (2021) Froth flotation of fluorite: a review. Adv Colloid Interface Sci 290:102382. https://doi.org/10.1016/j.cis.2021.102382

17. Jin S, Ou L, Ma X, Zhou H, Zhang Z (2021) Activation mechanisms of sodium silicate-inhibited fluorite in flotation under neutral and slightly alkaline conditions. Miner Eng 161:106738. https://doi.org/10.1016/j.mineng.2020.106738

18. Gao Z, Bai D, Sun W, Cao X, Hu Y (2015) Selective flotation of scheelite from calcite and fluorite using a collector mixture. Miner Eng 72:23–26. https://doi.org/10.1016/j.mineng.2014.12.025

19. Ai G, Zhou Y, Wang Y (2015) A study on the combined depressant for the Cu-S separation in low alkaline medium and its depressing mechanism. Procedia Eng 102:338–345. https://doi.org/10.1016/j.proeng.2015.01.156

20. Liu X, Luo H, Cheng R, Li C, Zhang J (2017) Effect of citric acid and flotation performance of combined depressant on collophanite ore. Miner Eng 109:162–168. https://doi.org/10.1016/j.mineng.2017.03.010

21. Feng B, Guo W, Xu H, Peng J, Luo X, Zhu X (2017) The combined effect of lead ion and sodium silicate in the flotation separation of scheelite from calcite. Sep Sci Technol 52:567–573. https://doi.org/10.1080/01496395.2016.1260590

22. Zhu W, Pan J, Yu X, He G, Liu C, Yang S, Zeng Y, Zeng A, Liu T (2021) The flotation separation of fluorite from calcite using hydroxypropyl starch as a depressant. Colloids Surfaces A Physicochem Eng Asp 616:126168. https://doi.org/10.1016/j.colsurfa.2021.126168

23. Ramirez DOS, Carletto RA, Tonetti C, Giachet FT, Varesano A, Vineis C (2017) Wool keratin film plasticized by citric acid for food packaging, Food Packag. Shelf. Life 12:100–106. https://doi.org/10.1016/j.fpsl.2017.04.004

24. Hashemikia S, Montazer M (2012) Sodium hypophosphite and nano TiO 2 inorganic catalysts along with citric acid on textile producing multi-functional properties. Appl Catal A Gen 417–418:200–208. https://doi.org/10.1016/j.apcata.2011.12.041

25. Gao Z, Gao Y, Zhu Y, Hu Y, Sun W (2016) Selective flotation of calcite from fluorite: a novel reagent schedule. Minerals 6:2–9. https://doi.org/10.3390/min6040114

26. Wei Q, Dong L, Jiao F, Qin W (2019) Use of citric acid and Fe(III) mixture as depressant in calcite flotation. Colloids Surfaces A Physicochem Eng Asp 578:123579. https://doi.org/10.1016/j.colsurfa.2019.123579

27. Liu J, Zeng Y, Ejtemaei M, Nguyen AV, Wang Y, Wen S (2019) DFT simulation of S-species interaction with smithsonite (0 0 1) surface: effect of water molecule adsorption position. Results Phys 15:102575. https://doi.org/10.1016/j.rinp.2019.102575

28. Han C, Li T, Zhang W, Zhang H, Zhao S, Ao Y, Wei D, Shen Y (2018) Density functional theory study on the surface properties and floatability of hemimorphite and smithsonite. Minerals 8:4–6. https://doi.org/10.3390/min8120542

29. Liu J, Wen S, Deng J, Chen X, Feng Q (2014) DFT study of ethyl xanthate interaction with sphalerite (1 1 0) surface in the absence and presence of copper. Appl Surf Sci 311:258–263. https://doi.org/10.1016/j.apsusc.2014.05.052

30. Liu J, Wang Y, Luo D, Zeng Y, Wen S, Chen L (2018) DFT study of SDD and BX adsorption on sphalerite (1 1 0) surface in the absence and presence of water molecules. Appl Surf Sci 450:502–508. https://doi.org/10.1016/j.apsusc.2018.04.194

31. Hu Y, Gao Z, Sun W, Liu X (2012) Anisotropic surface energies and adsorption behaviors of scheelite crystal. Colloids Surfaces A Physicochem Eng Asp 415:439–448. https://doi.org/10.1016/j.colsurfa.2012.09.038

32. Yang X, Roonasi P, Holmgren A (2008) A study of sodium silicate in aqueous solution and sorbed by synthetic magnetite using in situ ATR-FTIR spectroscopy. J Colloid Interface Sci 328:41–47. https://doi.org/10.1016/j.jcis.2008.08.061

33. Zhao J, Wang J, Qin X, Cao Y (2020) An ab-initio study of H2O adsorption on the calcite (104) surface with different coverages. Solid State Commun 313:113892. https://doi.org/10.1016/j.ssc.2020.113892

34. Ohnishi N, Yoshida S, Namba Y (2006) High resolution transmission electron microscopy study of calcium fluoride single crystal (111) surfaces processed by ultraprecision machining. Mater Trans 47:267–270. https://doi.org/10.2320/matertrans.47.267